Mice lacking Pctp/StarD2 exhibit increased adaptive thermogenesis and enlarged mitochondria in brown adipose tissue[s]

Hye Won Kang,* Scott Ribich,[1,†] Brian W. Kim,[2,†] Susan J. Hagen,[§] Antonio C. Bianco,[2,†] and David E. Cohen[3,*,**]

Department of Medicine, Division of Gastroenterology* and Division of Endocrinology,[†] Brigham and Women's Hospital, Harvard Medical School, Boston, MA; Department of Surgery,[§] Beth Israel Deaconess Medical Center, Boston, MA; and Division of Health and Sciences and Technology,** Harvard-Massachusetts Institute of Technology, Boston, MA

Abstract $Pctp^{-/-}$ mice that lack phosphatidylcholine transfer protein (Pctp) exhibit a marked shift toward utilization of fatty acids for oxidative phosphorylation, suggesting that Pctp may regulate the entry of fatty acyl-CoAs into mitochondria. Here, we examined the influence of Pctp expression on the function and structure of brown adipose tissue (BAT), a mitochondrial-rich, oxidative tissue that mediates nonshivering thermogenesis. Consistent with increased thermogenesis, $Pctp^{-/-}$ mice exhibited higher core body temperatures than wild-type controls at room temperature. During a 24 h cold challenge, $Pctp^{-/-}$ mice defended core body temperature efficiently enough that acute, full activation of BAT thermogenic genes did not occur. Brown adipocytes lacking Pctp harbored enlarged and elongated mitochondria. Consistent with increased fatty acid utilization, brown adipocytes cultured from $Pctp^{-/-}$ mice exhibited higher oxygen consumption rates in response to norepinephrine. The absence of Pctp expression during brown adipogenesis in vitro altered the expression of key transcription factors, which could be corrected by adenovirus-mediated overexpression of Pctp early but not late during the differentiation.█▌█ Collectively, these findings support a key role for Pctp in limiting mitochondrial oxidation of fatty acids and thus regulating adaptive thermogenesis in BAT.—Kang, H. W., S. Ribich, B. W. Kim, S. J. Hagen, A. C. Bianco, and D. E. Cohen. **Mice lacking phosphatidylcholine transfer protein/StarD2 exhibit increased adaptive thermogenesis and enlarged mitochondria in brown adipose tissue.** *J. Lipid Res.* **2009.** 50: 2212–2221.

Supplementary key words lipid binding protein • fatty acyl-CoA • fatty acid • brown adipocyte • thioesterase • phosphatidylcholine transfer protein

Phosphatidylcholine transfer protein (Pctp; also known as StarD2) is a soluble intracellular lipid binding protein that is specific for phosphatidylcholines. Pctp belongs to the steroidogenic acute regulatory protein-related transfer (START) domain superfamily of proteins (1, 2), which bind lipids and mediate intracellular transport, metabolism, and signaling (3–5). Whereas Pctp mediates intermembrane transfer of phosphatidylcholines in vitro (6), its biological function is uncertain (7).

We recently reported that $Pctp^{-/-}$ mice exhibit increased hepatic insulin sensitivity (8). This was associated with increases in body fat composition and turnover of triglycerides. In $Pctp^{-/-}$ mice, reduced respiratory quotients indicated preferential fatty acid utilization by oxidative tissues for energy production. Considering that expression levels of Pctp are accentuated in metabolically active tissues, including liver, heart, muscle, and kidney (7), these

Abbreviations: BAT, brown adipose tissue; GFP, green fluorescent protein; Nrf, nuclear respiratory factor; OCR, oxygen consumption rate; Pctp, phosphatidylcholine transfer protein; Pgc, peroxisome proliferator activate receptor γ coactivator; Ppar, peroxisome proliferator activate receptor; PK, protein kinase; Rpl32, L32 ribosomal protein; Tfam, mitochondrial transcription factor A; Them, thioesterase superfamily member; Ucp, uncoupling protein.

[1] Present address of S. Ribich: Sirtris Pharmaceuticals, Suite 300, 200 Technology Square, Cambridge, MA 02138.

[2] Present address of B. W. Kim and A. C. Bianco: Division of Endocrinology, Diabetes, and Metabolism, University of Miami Miller School of Medicine, Suite 816 Dominion Towers, 1400 NW 10th Ave., Miami, FL 33136.

[3] To whom correspondence should be addressed.
  e-mail: dcohen@partners.org

[s] The online version of this article (available at http://www.jlr.org) contains supplementary data in the form of one table.

findings support the notion that Pctp participates in regulating energy substrate utilization. Suggestive of a key role for Pctp in mitochondrial fatty acid metabolism (7, 9), yeast two-hybrid screening (10) has demonstrated that the mitochondrial-associated thioesterase superfamily member (Them) 2 (11, 12) is a Pctp-interacting protein. In this connection, Pctp stimulates the acyl-CoA thioesterase activity of Them2 in vitro (10, 12).

Brown fat, which is a mitochondrial-rich tissue that mediates nonshivering thermogenesis in the mouse (13), may also play important roles in human energy metabolism (14–16). Our finding that Pctp is expressed in mouse brown adipose tissue (BAT) prompted us to explore its influence on this oxidative tissue. In contrast to mice housed at thermoneutrality (30°C), $Pctp^{-/-}$ mice at room temperature exhibited higher core body temperatures compared with wild-type controls. They also preserved their core temperatures during cold exposure without full induction of thermogenic genes in BAT. Brown adipocytes lacking Pctp exhibited enlarged and elongated mitochondria. When cultured from $Pctp^{-/-}$ mice, mature brown adipocytes exhibited increased energy expenditure in response to norepinephrine. The expression of key transcription factors was attenuated during the differentiation of $Pctp^{-/-}$ preadipocytes in vitro but could be rescued by adenovirus-mediated overexpression of Pctp early during differentiation. These findings support a key role for Pctp in regulating adaptive thermogenesis and mitochondrial function.

MATERIALS AND METHODS

Animals

Wild-type and $Pctp^{-/-}$ littermate control mice on an FVB/NJ genetic background (8) were housed (two to five mice/cage) in an animal facility with a 12 h light/dark cycle and maintained on a standard rodent diet 5001 (LabDiets, St. Louis, MO). The temperature of the animal facility was maintained at 22 ± 1°C. Protocols for animal use and euthanasia were approved by the institutional committee of Harvard Medical School.

Protein expression in brown fat

Interscapular brown fat was dissected following CO_2-mediated euthanasia of 7–8 week old wild-type and $Pctp^{-/-}$ mice. The tissue was homogenized in RIPA buffer (1% NP-40, 0.5% sodium deoxycholate, 0.1% SDS, 150 mM NaCl, 50 mM Tris-HCl, and 2 mM EDTA). Protein expression in wild-type and $Pctp^{-/-}$ mice was assessed by Western blot analysis. Polyclonal antibodies to Pctp and Them2 were as described (10). A mouse monoclonal antibody to β-actin was from Sigma-Aldrich (St. Louis, MO). Detection of primary antibodies was with enhanced chemiluminescence (GE Healthcare Bio-Sciences, Piscataway, NJ) using goat anti-mouse (Sigma-Aldrich) or anti-rabbit horseradish peroxidase-conjugated secondary antibodies (Bio-Rad, Hercules, CA).

Responsiveness to temperature and norepinephrine administration

To determine the contribution of Pctp to adaptive thermogenesis, we compared 7–8 week old male wild-type and $Pctp^{-/-}$ mice housed at thermoneutrality (30°C) (17), at room temperature (23°C), or in the cold (4°C) (18). Mice were placed individually in plastic cages with minimal amounts of bedding. To achieve thermoneutrality, cages containing wild-type and $Pctp^{-/-}$ mice were placed in a clean, ventilated, and temperature-controlled incubator for 48 h (Fisher Scientific, Pittsburgh, PA). For room temperature and cold exposure studies, mice were kept for 24 h in the laboratory and cold room, respectively. Prior to and periodically during the experiments, core body temperature was measured using a rectal probe connected to a YSI precision 4000A thermometer (Measurement Specialties, Hampton, VA). In a separate study, mice at thermoneutrality were injected subcutaneously with 1 µg/g of 0.5 mg/ml L-(−)-norepinephrine-(+) bitartrate (Calbiochem, San Diego, CA) dissolved in 150 mM NaCl and 0.3 mM ascorbic acid. Based on preliminary experiments, a period of 4 h following injection was chosen for harvesting brown fat because it allowed for maximal upregulation of Ucp1 mRNA in wild-type mice. Upon completion of experiments, mice were euthanized by CO_2 gas. Interscapular brown fat pads were immediately excised, snap frozen in liquid nitrogen, and stored at −80°C.

Ultrastructural analysis of brown fat

Brown fat freshly harvested from 7–8-week-old mice was prepared for electron microscopy (19). Briefly, samples were fixed by immersion using 2.5% glutaraldehyde, 1.25% formaldehyde, and 0.03% picric acid in 0.1 M sodium cacodylate buffer (pH 7.4) for 1 h at room temperature. Tissues were postfixed for 1 h with 1% osmium tetroxide and 1.5% potassium ferrocyanide in cacodylate buffer and then by aqueous 1% uranyl acetate for 30 min, both at room temperature. Following dehydration in ethanol and propylene oxide, tissues were embedded in LX112 resin (Ladd Research Industries, Burlington, VT). Ultrathin sections were cut using a Leica Ultracut E ultramicrotome (Leica Microsystems, Deerfield, IL), placed on formvar- and carbon-coated grids, stained with uranyl acetate and lead citrate, and then imaged with a JEOL 1200EX transmission electron microscope (JEOL USA, Peabody, MA). Images were prepared from processed film using an Epson scanner (Epson America, Long Beach, CA). Identification of the developmental stages of brown adipocytes was as described (20).

Mitochondrial size and shape were quantified using blocks prepared from brown fat excised from two $Pctp^{-/-}$ and two wild-type mice. Each grid was photographed at 5,000× magnification in five distinct grid space locations: one central plus four outer quadrants. The qualifications for a photograph to be taken were that the nucleus must be observed in the plane and be included with cytoplasm and that the cell must contain adequate cytoplasm in the image so that mitochondria would be present. For wild-type mice, four photographs were taken in each grid space location. Because preliminary experiments in $Pctp^{-/-}$ mice revealed that mitochondrial sizes were more polydisperse and that there were more developing and degenerating cells present, three grid spaces were analyzed in each location, and each grid space was photographed in two locations. The electron microscope was calibrated using a carbon grating replica, and photographs were scanned and analyzed in digital format (21). Final magnifications were determined as the products of microscope magnification each day that photographs were taken. Near the center of each photograph, 8–11 contiguous mitochondria were selected for analysis. Because mitochondria in developing brown adipocytes exhibit distinct characteristics (20), we restricted our analysis to those contained within mature brown adipocytes. The perimeter of each mitochondrion was traced using the magnetic lasso tool of Adobe Photoshop CS4 Extended Version (Adobe Systems, San Jose, CA). For each mitochondrion, the computer algorithm calculated height (h = maximal dimension, µM), width (w = minimal dimension, µm), area (µm^2), and perimeter (µm). Values

were averaged for each photomicrograph, and means of average values were determined for wild-type and $Pctp^{-/-}$ mice. In order to determine the shape of mitochondria, empirically determined values for the area and perimeter were compared with geometrically calculated using measured values of h and w: For an ellipse, area $= \pi ab$ and perimeter $\approx 2\pi((a^2 + b^2)/2)^{1/2}$, where $a = h/2$ and $b = w/2$. This formula for perimeter represents an approximation that applies for h < 3w, which was appropriate for our data. Mitochondrial mass of brown fat of wild-type and $Pctp^{-/-}$ mice was also estimated biochemically by measuring citrate synthase activity (22).

Primary culture and differentiation of brown preadipocytes

Primary brown preadipocytes were isolated from interscapular brown fat of 4–5 week old wild-type and $Pctp^{-/-}$ mice, cultured, and differentiated (18, 19). Briefly, brown fat was surgically removed from mice (8–10 mice per group) euthanized by CO_2 asphyxiation. The dissected tissues were pooled, minced, and digested with collagenase (Sigma-Aldrich) and dissolved in media containing DMEM, 10 mM HEPES, and antibiotics (25 µg/ml streptomycin, 25 µg/ml tetracycline, 25 µg/ml ampicillin, and 0.8 µg/ml fungizone). Cells were strained to remove tissue debris, plated in BD 75 cm^2 T-flasks (BD Biosciences, San Jose, CA), and incubated (37°C, 5% CO_2) for 5–6 days in the same media plus 10% (v/v) FBS and 3 nM insulin. After this initial period, cells were trypsinized and seeded in BD 6-well plates (BD Biosciences) at density of 17,500 cells/cm^2 in culture medium. When cells achieved confluence (typically after 3 d), differentiation of the preadipocytes was initiated by addition to the media of 500 µM isobutylmethylxanthine, 2 µg/ml dexamethasone, and 125 µM indomethacin. After 2 days, the media were replaced with the same media lacking these three components, and the cells were cultured for 6 days. Differentiation of preadipocytes into mature brown adipocytes was confirmed by the presence of multilocular lipid droplets in the cytosol by light microscopy. In selected experiments, adenoviral vectors were utilized to overexpress Pctp or green fluorescent protein (GFP) during differentiation of brown adipocytes. Recombinant mouse Pctp adenovirus (Ad-CMV-Pctp) was constructed by standard techniques utilizing the open reading frame of a mouse Pctp cDNA (ViraQuest, North Liberty, IA). A recombinant GFP adenovirus (Ad-CMV-GFP) was used as a control. On days 1, 5, 7, 9, and 11 following plating of preadipocytes, Ad-CMV-Pctp or Ad-CMV-GFP was added to the media and exposed to primary brown adipocytes in culture at a multiplicity of infection of 3 for 3 h.

Quantitative PCR analysis of gene expression

Total RNA was extracted from brown fat or primary brown adipocytes using TRIzol (Invitrogen, Carlsbad, CA), treated with DNaseI to remove genomic DNA, and then purified using an RNeasy Mini kit (Qiagen, Valencia, CA). cDNA was synthesized using the SuperScript III first-strand synthesis system for RT-PCR (Invitrogen). Gene expression was quantified using LightCycler FastStart DNA Master^{plus} SYBR Green I (Roche Applied Sciences, Indianapolis, IN) in a LightCycler 1.5 (Roche Applied Sciences). Gene-specific primers were designed using the web-based software Primer3 (http://frodo.wi.mit.edu/cgi-bin/primer3/primer3_www.cgi) and are listed in supplementary Table I. The L32 ribosome protein (Rpl32) was used as an invariant gene (8).

Fluorescence microscopy

Lipid droplets in primary brown adipocytes were visualized by fluorescence microscopy (23). Fully differentiated primary brown adipocytes were washed with PBS, fixed with 4% paraformalde-

hyde for 20 min, and then washed 3 × 5 min with PBS. Cells were then permeabilized by exposure to 0.2% Triton X-100 for 20 min. After washing with PBS, cells were incubated for 2 h with 10 µg/ml BODIPY 493/503 (Molecular Probes, Eugene, OR) diluted in PBS that contained 1% BSA. Washed cells were mounted and lipid droplets were visualized using an Eclipse TE200 fluorescence microscope (Nikon, Melville, NY) fitted with a Roper Scientific Photometrics Coolsnap ES CCD camera (Princeton Instruments, Trenton, NJ).

Cellular oxygen consumption

Primary brown preadipocyte cells were seeded at density of 17,500 cells/cm^2 into customized Seahorse 24-well plates (Seahorse Bioscience, North Billerica, MA), which consisted of wells with surface areas equivalent to standard 96-well plates. Once fully differentiated as described above, the media was replaced with prewarmed XF24 assay media for 1 h; this unbuffered media consisted of DMEM (Sigma-Aldrich), 1 mM Glutamax-1 (Invitrogen), 2 mM pyruvate, 141 mM NaCl, and 25 mM glucose. Measurements of cellular O_2 consumption were performed (24) using an XF24 Extracellular Flux Analyzer (Seahorse Bioscience). The XF24 device measured O_2 tension using optical fluorescent biosensors embedded in a sterile disposable cartridge, which was placed into the wells of the microplate during the assay and created an ~7 µl "microenvironment" above the cells. O_2 consumption rate (OCR) was calculated by plotting the O_2 tension of media in the microenvironment as a function of time (pmol/min). Data were normalized by the protein concentration present in each individual well. In some experiments, cells were exposed to L-(−)-norepinephrine-(+) bitartrate or insulin (Sigma-Aldrich).

Statistical analysis

Data are presented as mean ± SEM. Comparisons were assessed using two-tailed unpaired Student's t-test or ANOVA using a Bonferroni post test analysis (Prism 5; GraphPad Software, La Jolla, CA). For measurements of mitochondrial morphology, parameters were compared by the Mann-Whitney rank sum test due to either unequal variances or nonnormal distributions. Differences were considered significant for $P < 0.05$.

RESULTS

Expression of Pctp and Them2 in brown fat

Figure 1 demonstrates the expression of Pctp as well as Them2 in the brown fat of wild-type and $Pctp^{-/-}$ mice. Pctp protein was expressed in brown fat of wild-type mice, but not $Pctp^{-/-}$ mice. Them2 was also expressed in brown fat, and its expression increased modestly in the absence of Pctp expression.

Adaptive thermogenesis and cold tolerance in $Pctp^{-/-}$ mice

Figure 2 shows the influence of Pctp expression on core body temperature of mice maintained at thermoneutrality, room temperature, or subjected to the cold. When mice were separated and placed in individual cages at 30°C (Fig. 2A), core body temperatures in $Pctp^{-/-}$ mice did not change. By contrast, in wild-type mice temperatures declined by >1°C over the first 2 h and then gradually increased. Core body temperatures of wild-type mice were significantly lower at 2 and 4 h, and differences approached
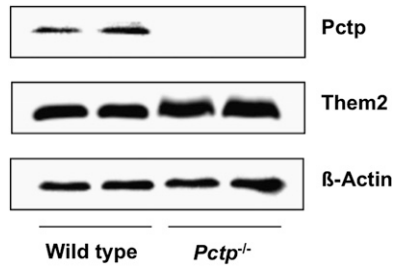
Fig. 1. Expression of Pctp and Them2 in brown fat. Western blot analysis using homogenates of brown fat harvested from FVB/NJ wild-type and $Pctp^{-/-}$ mice. The blot was also probed with β-actin to verify equal loading.

significance at 3 h ($P = 0.051$) and 24 h ($P = 0.056$). By 48 h, body temperatures of wild-type mice returned to baseline and were not different from $Pctp^{-/-}$ mice. For mice housed at room temperature (Fig. 2B), separation into individual cages was associated with modest but significant decreases in core body temperatures of both wild-type and $Pctp^{-/-}$ mice. While not different initially, core body temperatures (°C) were higher in $Pctp^{-/-}$ compared with wild-type mice at the end of the 24 h period (wild type, 37.25 ± 0.05; $Pctp^{-/-}$, 37.67 ± 0.10). For mice placed in the cold

(Fig. 2C), there was an initial decrease of ~2°C in core body temperature over the first 4 h for both genotypes, which then leveled off for the remainder of the 24 h period. Core body temperatures were similar for wild-type and $Pctp^{-/-}$ mice throughout, and all survived the cold challenge.

Figure 3 displays the influence of temperature and Pctp expression on mRNA levels of selected key genes that play roles in brown fat function as well as the Pctp-interacting protein Them2. As shown in Fig. 3A, Pctp mRNA in brown fat was strongly upregulated as a function of decreasing temperature. Them2 was upregulated more modestly in wild-type mice, but to a greater extent than in $Pctp^{-/-}$ mice (Fig. 3B). At thermoneutrality, uncoupling protein 1 (Ucp1) mRNA expression (Fig. 3C) was 0.74-fold lower in $Pctp^{-/-}$ compared with wild-type mice. Values for Ucp1 were the same at room temperature but were again lower after $Pctp^{-/-}$ mice were housed for 24 h in the cold. At thermoneutrality and at room temperature, steady state mRNA expression levels of peroxisome proliferator activate receptor (Ppar) γ coactivator 1α (Pgc1a) were similar in wild-type and $Pctp^{-/-}$ mice (Fig. 3D), and there was modest induction at room temperature compared with thermoneutrality. Whereas cold exposure strongly in-
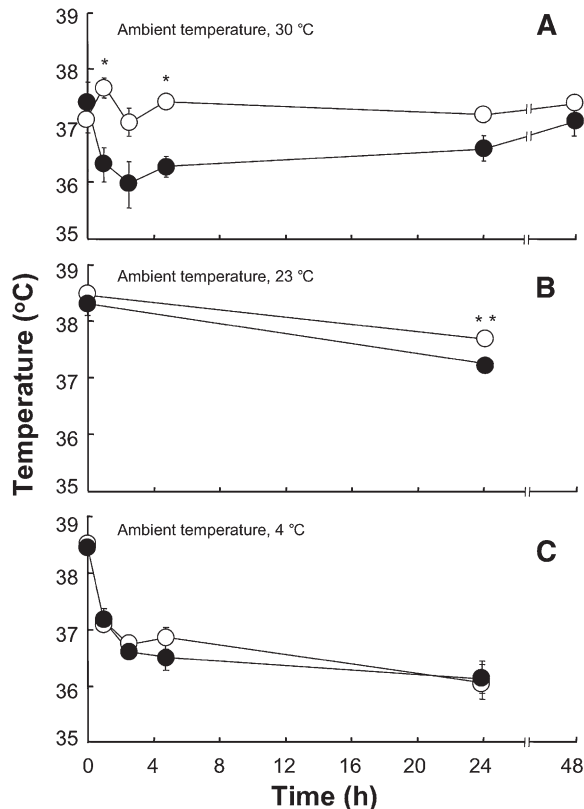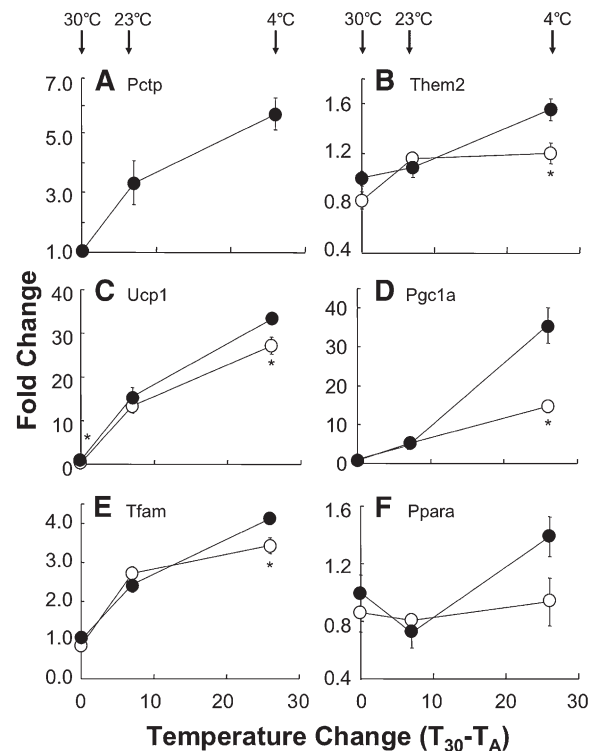

Fig. 2. Influence of Pctp expression and ambient temperature on core body temperatures of mice. Core body temperature was measured for wild-type (closed circles) and $Pctp^{-/-}$ (open circles) mice maintained at 30°C (A; wild type, n = 5; $Pctp^{-/-}$, n = 5), 23°C (B; wild-type, n = 7; $Pctp^{-/-}$, n = 11), and 4°C (C; wild type, n = 6; $Pctp^{-/-}$, n = 9). Where not visible, error bars are contained within symbol sizes. *$P < 0.05$, $Pctp^{-/-}$ versus wild type; **$P < 0.006$, $Pctp^{-/-}$ versus wild-type.

Fig. 3. Attenuated thermal stress-induced gene induction in brown fat of $Pctp^{-/-}$ mice. Upon conclusion of the experiments in Fig. 2, gene expression was measured in brown fat harvested from wild-type (closed circles) and $Pctp^{-/-}$ (open circles) mice (n = 4/group). Expression levels were normalized to values for wild type at 30°C and fold changes plotted as functions of the magnitude of ambient temperature (T_A) reductions below 30°C ($T_{30} - T_A$) for Pctp (A), Them2 (B), Ucp1 (C), Pgc1a (D), Tfam (E), and Ppara (F). The arrows indicate T_A for each experiment. Where not visible, error bars are contained within symbol sizes. *$P < 0.05$, $Pctp^{-/-}$ versus wild type.

duced Pgc1a in wild-type mice, there was much more modest induction in the absence of Pctp expression. Because Ucp1 and Pgc1a are both induced by adrenergic stimulation (25), the influence of Pctp expression on mRNA for these genes was also examined following subcutaneous administration of norepinephrine to mice at thermoneutrality. In mice lacking Pctp, norepinephrine-induced upregulation of mRNA (fold change, n = 5/group) was not impaired for either Ucp1 (wild type, 2.5 ± 0.3; $Pctp^{-/-}$, 1.8 ± 0.3) or Pgc1a (wild type, 2.1 ± 0.2; $Pctp^{-/-}$, 1.8 ± 0.3). For mitochondrial transcription factor A (Tfam; Fig. 3E) and Ppara (Fig. 3F), there were also no differences in mRNA expression between wild-type and $Pctp^{-/-}$ mice housed at thermoneutrality and room temperature. However, following cold exposure, Tfam mRNA expression was higher in wild-type mice and tended to be higher for Ppara ($P = 0.08$). For Pparg and nuclear respiratory factor 1 (Nrf1), mRNA levels were induced by decreases in ambient temperature but were not appreciably different in wild-type and $Pctp^{-/-}$ mice (data not shown).

Influence of Pctp expression on function of cultured primary brown adipocytes

We next examined in vitro whether Pctp expression might influence the phenotypic characteristics of brown adipocytes. Primary preadipocytes were cultured from brown fat of wild-type and $Pctp^{-/-}$ mice and then differentiated over 11 days (18). **Figure 4** displays fluorescence micrographs of brown adipocytes following BODIPY staining, which allows visualization of lipid droplets. Cells from both wild-type mice (Fig. 4A) and $Pctp^{-/-}$ mice (Fig. 4B) exhibited multiple lipid droplets of varied sizes, a characteristic feature of brown adipocytes. The appearance and abundance of cells as well as lipid droplets were not influenced appreciably by the absence of Pctp expression.

To assess functional differences, we measured cellular respiration via XF24 extracellular flux analyzer (Fig. 4C, D). There was no difference in basal OCR (pmol/min/mg protein) of cultured brown adipocytes (wild type, 244 ± 21; $Pctp^{-/-}$, 254 ± 22). However, in the absence of Pctp expression, the addition of norepinephrine resulted in a much more robust increase in OCR values (Fig. 4C). Under similar experimental conditions, the addition of insulin tended to reduce values of OCR modestly, most likely as a result of accelerated glycolysis. However, there were no differences attributable to Pctp expression (Fig. 4D).

Influence of Pctp expression on gene expression during differentiation of cultured primary brown preadipocytes

Figure 5 demonstrates the influence of Pctp on gene expression during the in vitro differentiation of brown preadipocytes. Figure 5A displays the induction of gene expression on day 11 compared with day 2 in brown preadipocytes cultured from wild-type mice. The expression of each gene increased, with magnitudes of induction that ranged broadly from 1.2-fold for Nrf1 to 1600-fold for Pparg. Pctp and Them2 were upregulated 5.8- and 2.9-fold, respectively. The absence of Pctp had a substantial impact on gene expression (Fig. 5B). Compared with the wild type, preadipocytes lacking Pctp tended to express lower mRNA levels of Pgc1a, Pparg, and Ppara. In mature brown adipocytes cultured from $Pctp^{-/-}$ compared with wild-type mice, levels of Pgc1a, Pparg, Ppara, Ucp1, and Tfam were lower (Fig. 5B, inset). Levels of Them2 in mature brown adipocytes were slightly, but not significantly, reduced by the lack of Pctp expression, which is in keeping with our recent observation that it is a target gene of Ppara (12).

Influence of Pctp expression on the ultrastructure of brown fat

Considering that brown fat is rich in mitochondria and utilizes fatty acids at a high rate, we explored whether
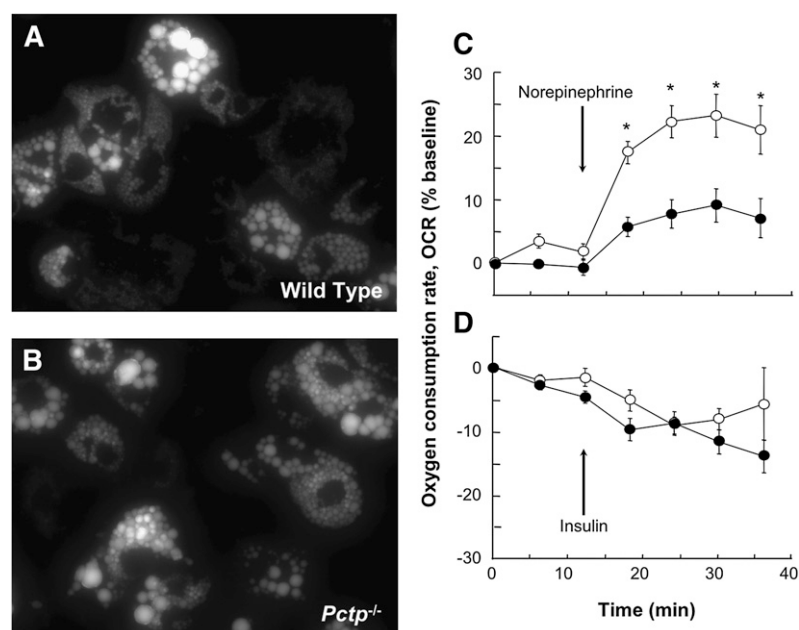

Fig. 4. Normal appearance of lipid droplets but increased norepinephrine responsiveness in cultured brown adipocytes from $Pctp^{-/-}$ mice. Fluorescence microscopy was performed following BODIPY staining of fully differentiated brown adipocytes (day 11) cultured from wild-type (A) and $Pctp^{-/-}$ (B) mice. Following an initial equilibration period, 10 μM norepinephrine (C) or 10 nM insulin (D) were added, as indicated by the arrows. OCR was determined for differentiated primary brown adipocytes from wild-type (closed circles) and $Pctp^{-/-}$ (open circles) mice. Data points represent means of 10 wells and are representative of two independent experiments. Where not visible, error bars are contained within symbol sizes. * $P < 0.05$, $Pctp^{-/-}$ versus wild type.
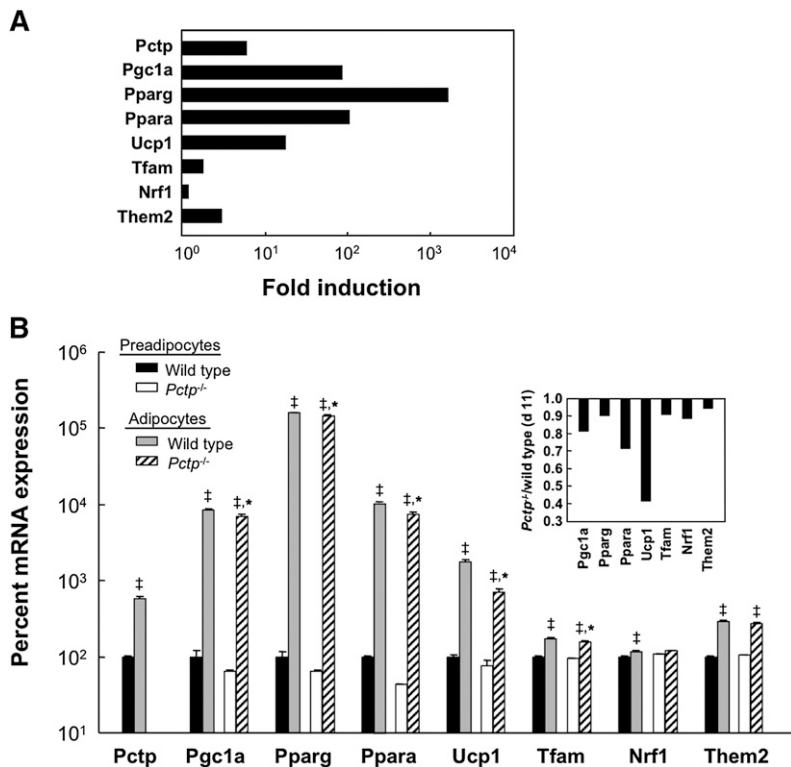
Fig. 5. Absence of Pctp expression alters gene expression during differentiation of brown preadipocytes in vitro. A: Fold changes in expression of selected genes during differentiation of wild-type brown preadipocytes into mature brown adipocytes. Data represent expression of mRNA in differentiated brown adipocytes on day 11 relative to expression prior to differentiation on day 2 and are plotted on a logarithmic scale. B: Influence of Pctp on gene expression in brown preadipocytes (black bars, wild type; white bars, $Pctp^{-/-}$) and in mature brown adipocytes (gray bars, wild type; cross-hatched bars, $Pctp^{-/-}$). $^{\ddagger}P < 0.05$, adipocytes versus preadipocytes, $^{*}P < 0.05$, $Pctp^{-/-}$ versus wild type. Measurements were performed in duplicate on each RNA sample of two RNA samples per group and plotted on a logarithmic scale. For each gene, the inset demonstrates the ratio of the mean mRNA expression on day 11 for $Pctp^{-/-}$ mice to mean expression for wild-type mice on day 11. Values of mRNA expression were obtained by normalizing to mRNA levels of a reference gene (Rpl32).

there were ultrastructural changes in brown fat that might provide insights into the alterations in energy substrate utilization previously observed in $Pctp^{-/-}$ mice (8) as well as the increased capacity to generate heat and respond to norepinephrine observed in the absence of Pctp expression. **Figure 6** demonstrates electron microscopy images of brown fat. Brown fat from wild-type mice consisted of large mature adipocytes that contained mitochondria and numerous lipid droplets, and each cell was in close proximity to capillaries within the small intercellular connective tissue space (Fig. 6A). Lipid droplets in these mature brown adipocytes were of variable size. Brown fat from $Pctp^{-/-}$ mice contained some adipocytes with similar characteristics to wild-type cells, but overall many cells had larger lipid droplets; the lipid droplets appeared to fuse into very large structures that occupied much of the cell cytoplasm (Fig. 6B).

In contrast to control mice, brown fat from $Pctp^{-/-}$ mice had numerous developing brown adipocytes (20), including protoadipocytes (Fig. 6B) and preadipocytes (Fig. 6C). Protoadipocytes had a large nuclear to cytoplasmic ratio, a pale cytoplasm, and contained a few small lipid droplets (Fig. 6B). Preadipocytes contained small mitochondria that had a dense matrix and numerous lipid droplets (Fig. 6C, D). Additionally, both mitochondria and lipid droplets in preadipocytes were surrounded by smooth endoplasmic reticulum (Fig. 6D). Mitochondria in mature brown adipocytes from wild-type mice were predominantly ellipsoid in shape, with a pale matrix and numerous well-organized cristae (Fig. 6A, E). By contrast, the mitochondria in adipocytes from $Pctp^{-/-}$ mice were considerably larger with a greater number of cristae that were arranged in a parallel fashion (Fig. 6F). Figure 6G and H illustrates

an additional prominent feature of brown fat from $Pctp^{-/-}$ mice that was not observed in wild-type mice; there were many degenerating adipocytes that had an electron dense cytoplasm when compared with surrounding cells (Fig. 6G). Within the cytoplasm of these degenerating cells, mitochondria had an abnormal structure with disrupted cristae (Fig. 6H). Macrophages could also be seen in the intercellular connective tissue space between degenerating brown adipocytes in $Pctp^{-/-}$ mice (Fig. 6H).

We next quantified the morphologic characteristics for 402 mitochondria from wild-type mice and 642 mitochondria from $Pctp^{-/-}$ mice (**Fig. 7**). Enlargement of mitochondria in mature brown adipocytes in the absence of Pctp expression was evidenced by highly significant ($P < 0.001$) increases in mean height (μM) by 25% (wild type, 1.27 ± 0.02; $Pctp^{-/-}$, 1.59 ± 0.04) and mean width (μM) by 15% (wild type, 1.10 ± 0.02; $Pctp^{-/-}$, 1.28 ± 0.03) as well as a 34% increase in mean area (Fig. 7A). The greater increase in height compared with width is also indicative that mitochondria were more elongated in the absence of Pctp expression. Consistent with their elliptical appearances in both wild-type and $Pctp^{-/-}$ mice, calculated areas for an ellipse using the measured mean values of height and width were very close to empirically determined mean values for area, as illustrated in Fig. 7A. Figure 7B demonstrates that values of perimeter of mitochondria were 21% higher in $Pctp^{-/-}$ mice. Whereas for wild-type mice, the mean calculated value of perimeter based on height and width was only slightly higher (7.5%) than the measured value, the calculated value of perimeter for $Pctp^{-/-}$ mice was 50% higher. This suggests substantially more irregular perimeters of mitochondria in $Pctp^{-/-}$ mice. Although mitochondria contained within mature brown adipocytes
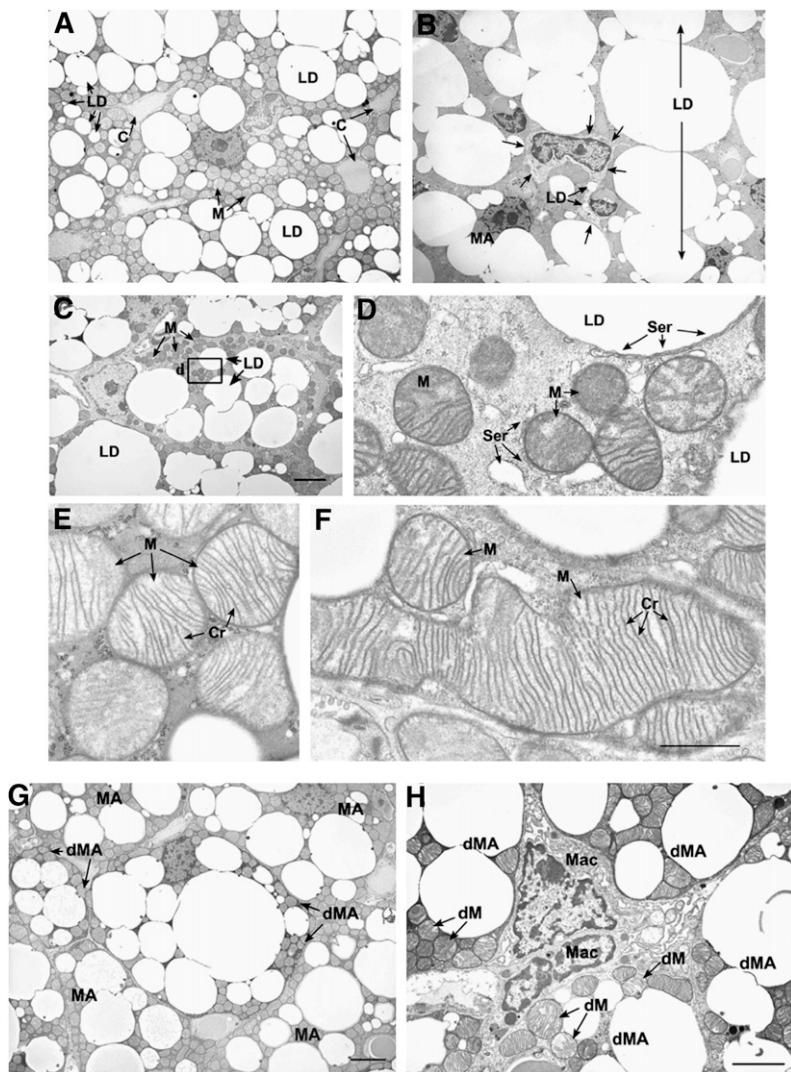
Fig. 6. Influence of Pctp expression on the ultra-structure of brown fat. The top series of electron micrographs show that the absence of Pctp expression leads to the presence of immature adipocytes and mitochondrial changes in brown fat. Characteristics of brown fat from wild-type (A, E) or $Pctp^{-/-}$ mice (B, C, D, F). A: Mature brown adipocytes in wild-type mice. LD, lipid droplet; C, blood capillary; M, mitochondria. B: Developing protoadipocyte at the same magnification as in A. LD, lipid droplet (two in protoadipocyte and one large fused large droplet); MA, mature adipocytes. Arrows mark the boundary of the protoadipocyte. C: Developing preadipocyte at the same magnification as in A. LD, lipid droplet; M, mitochondria. Bar in C applies to A–C and represents 4 µm. D: High magnification of the area in the box in C. Note that smooth endoplasmic reticulum (Ser) is found along the edge of the lipid droplet (LD), surrounding mitochondria (M), and in the cell cytoplasm. E: Mitochondria from control adipocytes (in A). Note that mitochondria (M) have a pale matrix and numerous cristae (Cr) that are well organized. F: Mitochondria from $Pctp^{-/-}$ mouse that is the same magnification as in E. Note the large size of mitochondria (M) and the large number of parallel cristae (Cr). Bar in F applies to D–F and represents 1 µm. The bottom pair of electron micrographs demonstrates that degenerating adipocytes are present in brown fat from $Pctp^{-/-}$ mice. G: Degenerating mature adipocytes (dMA) were found among mature adipocytes (MA) in the brown fat from $Pctp^{-/-}$ mice. The cytoplasm of degenerating brown adipocytes is electron dense in comparison to mature adipocytes. Bar represents 4 µm. H: The intercellular space between degenerating mature adipocytes (dMA) in brown fat from $Pctp^{-/-}$ mice is expanded, and macrophages (Mac) can be found in close association with the degenerating cells. In addition to electron-dense cytoplasm in degenerating mature adipocytes, mitochondria have an abnormal structure with disrupted cristae, pale matrix, and defects in shape (dM). Bar represents 6 µm.

were larger in $Pctp^{-/-}$ mice, citrate synthase activity (nmol/mg/min) in brown fat homogenates did not differ (wild type, 726 ± 108; $Pctp^{-/-}$, 827 ± 52).

Influence of Pctp overexpression during differentiation of cultured primary brown preadipocytes

In order to ascertain whether the altered pattern of gene expression observed in mature brown adipocytes could be reversed by reintroduction of the protein, Pctp was overexpressed in cultured brown adipocytes at various stages of differentiation (**Fig. 8**). Using Ad-CMV-Pctp, similar degrees of overexpression of mRNA on day 11 were achieved in wild-type and $Pctp^{-/-}$ cells compared with wild-type cells infected with Ad-CMV-GFP (Fig. 8A), with maximal adenoviral-mediated Pctp mRNA expression observed when cells were infected on day 7. GFP mRNA yielded the same pattern of expression as Pctp infection, and infection with either adenovirus did not influence the formation of lipid droplets in mature brown adipocytes of either genotype (data not shown). Figure 8B compares relative changes of mRNA expression of genes in $Pctp^{-/-}$ compared with wild-type adipocytes on day 11. Gene expression in Ad-CMV-Pctp-infected cells was normalized to

expression level in brown adipocytes infected with Ad-CMV-GFP. Fold change was then determined by comparison with expression on day 2. This revealed that Pgc1a, Pparg, and Ppara were induced to a greater degree in the absence of Pctp expression. Ucp1, Tfam, and Them2 were
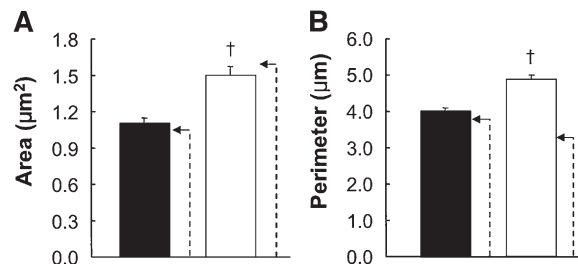

Fig. 7. Enlarged, elongated, and irregular mitochondria in mature brown adipocytes in BAT from $Pctp^{-/-}$ mice. Mitochondria in mature brown adipocytes in brown fat from two wild-type mice (closed bars) and two $Pctp^{-/-}$ mice (open bars) were analyzed by electron microscopy in order to quantify area (A) and perimeter (B). The dashed arrows indicate calculated values using means of height and width (see text) based on the assumption that mitochondria were elliptical. $^{†}P < 0.001$, $Pctp^{-/-}$ versus wild-type.
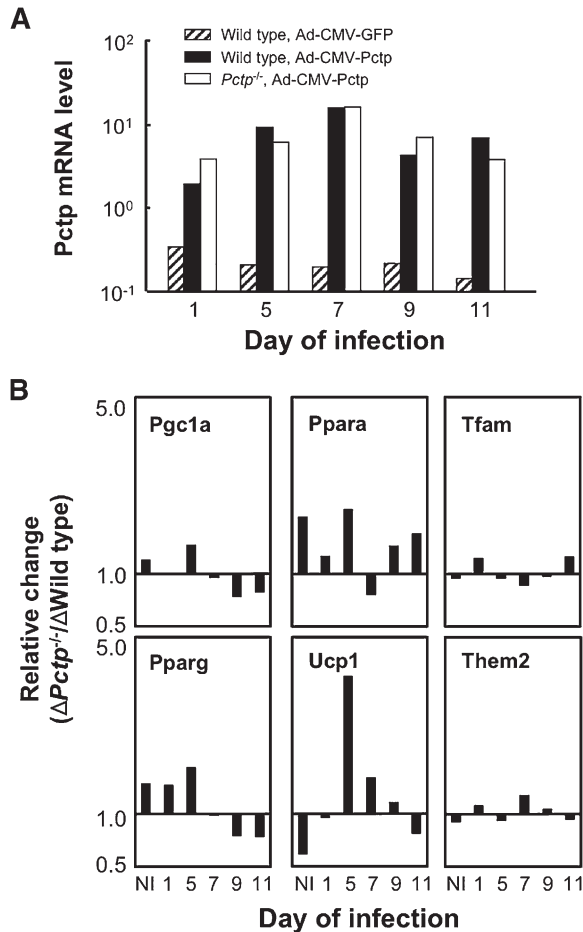
Fig. 8. Influence of Pctp overexpression on differentiation of brown adipocytes. A: Expression levels of Pctp mRNA on day 11 for wild-type cells infected with Ad-CMV-GFP (hatched bars) or Ad-CMV-Pctp (closed bars) and $Pctp^{-/-}$ cells infected with Ad-CMV-Pctp (open bars). Relative mRNA expression values were obtained by normalizing to expression of the reference gene, Rpl32, and are plotted on a logarithmic scale. B: Influence of Pctp overexpression on gene induction. Relative changes are expressed as the ratio of fold induction for $Pctp^{-/-}$ brown adipocytes (Fold $\Delta Pctp^{-/-}$) to the fold induction of wild-type mice (Fold Δwild-type) for each transcript. Gene expression relative to Rpl32 was normalized by expression of the same gene in cells infected on the same day with Ad-CMV-GFP relative to Rpl32. Fold induction was calculated as the ratio of fold change on day 11 following differentiation relative to expression on day 2 prior to differentiation and are plotted on a logarithmic scale. NI indicates no adenoviral infection.

less induced, as was Nrf1 (data not shown). For the genes with the largest relative changes in $Pctp^{-/-}$ versus wild-type brown adipocytes during differentiation in noninfected cells (i.e., Pgc1a, Ppara, Ucp1, and Pparg), overexpression of Pctp on day 1 sharply reduced relative changes in induction of Pgc1a, Ppara, Ucp1, and to a slight degree, Pparg. Overexpression of Pctp at later points in time also had substantial but highly varied effects of the relative changes of these genes. By contrast, overexpression of Pctp at any time point had little effect on induction of Tfam and Them2, as well as Nrf1 (data not shown). These were the genes for which the lack of Pctp expression had only a minor influence on induction during differentiation (Figure 5B).

DISCUSSION

This study was motivated by the observation that $Pctp^{-/-}$ mice utilize fatty acids almost exclusively as an energy substrate (8). Because in small animals, brown fat consumes half or more of calories and oxygen (13), we reasoned that BAT physiology might yield key insights into metabolic regulation in $Pctp^{-/-}$ mice. Our results indicate that Pctp expression regulates mitochondrial biology, thermogenesis, as well as differentiation of brown fat.

Although accentuated Pctp expression is generally observed in oxidative tissues (7), its presence in brown fat had not previously been demonstrated. Consistent with a putative role in oxidative metabolism and thermogenesis, Pctp was readily detected in brown fat. By contrast, it is not expressed in white fat (26). Based on the observation that Pctp stimulates the acyl-CoA thioesterase activity of Them2, we hypothesized that an interaction between these two proteins may regulate the access of fatty acyl-CoA molecules to mitochondria (10). This possibility is consistent with the findings that Them2 was robustly expressed in brown fat and that Pctp and Them2 in wild-type mice were upregulated both by cold exposure and during differentiation of cultured brown adipocytes.

Evidence for increased thermogenesis in $Pctp^{-/-}$ mice became apparent when litters were separated and placed in individual cages. Time-dependent decreases in core body temperatures for mice housed at thermoneutrality and room temperature were consistent with conditions of reduced housing density and minimal bedding (27, 28). Higher core body temperatures indicate that an increase in energy expenditure accompanied the previously described shift to fatty acid oxidation, which was evidenced by reduced respiratory quotients in $Pctp^{-/-}$ mice (8). However, in that study, we also reported that oxygen consumption rates (VO_2, ml/h/kg body weight) did not differ between wild-type and $Pctp^{-/-}$ mice housed under similar conditions. The apparent discrepancy is attributable to the normalization of VO_2 values to total weights, which did not differ between genotypes. This did not take into account that adiposity was increased in mice lacking Pctp and lean body mass (percentage of body weight) was reduced ($Pctp^{-/-}$, 76.5 ± 1.6; wild type, 85.4 ± 1.4). Appreciating that white adipose tissue does not contribute significantly to energy expenditure, indirect calorimetry measurements more precisely reflect lean body mass. Recalculation of EC_{50} values by percent relative cumulative frequency analysis (29) using data normalized to lean body mass revealed a 13% increase in VO_2 ($Pctp^{-/-}$, 5,556 ± 7; wild type 4,926 ± 13) and a 3% decrease in VCO_2 in $Pctp^{-/-}$ mice ($Pctp^{-/-}$, 3,887 ± 4; wild type, 3,991 ± 2). Renormalization of the data did not alter respiratory quotients (i.e., VCO_2/VO_2). Caloric intake, which did not differ between genotypes (8), was also 12% higher in $Pctp^{-/-}$ mice when adjusted for lean body mass. When taken together, these data are consistent with the increase in energy expenditure observed in this study.

An important trigger of thermogenesis in response to cold is sympathetic nervous system-mediated release of

norepinephrine (13). Stimulation of β_3-adrenergic receptors in BAT increases cAMP and activates protein kinase (PK) A. This both upregulates and phosphorylates Pgc1a, which promotes the transcription of Nrf1. Nrf1 induces key respiratory chain components as well as Tfam. Tfam translocates to mitochondria and promotes transcription of mitochondrial genes. PKA activation also leads to Ucp1 upregulation and to hydrolysis of triglycerides (13, 30). Upregulation of Ppara contributes to thermogenesis by increasing fatty acid oxidation (31).

Compared with wild-type controls, $Pctp^{-/-}$ mice defended body temperature more effectively at room temperature and equally effectively in the cold, but with lower induction of Ucp1, Pgc1a, Tfam, and Ppara. Because both Ucp1 and Pgc1a were fully upregulated by norepinephrine administration, their reduced upregulation in response to thermal stress likely reflects reduced sympathetic stimulation. These findings suggest that the absence of Pctp expression increased the efficiency of BAT, so that thermal homeostasis was achieved without full transcriptional activation of thermogenic genes. However, alternative explanations are also possible. $Pctp^{-/-}$ mice may harbor larger total BAT mass. Although there were no apparent differences in interscapular brown fat pad sizes (wild type, 0.21 ± 0.02 g; $Pctp^{-/-}$, 0.20 ± 0.02 g) attributable to Pctp expression, we have not explored the possibility that other BAT depots were increased in size or whether there might have been ectopic expression of brown fat in $Pctp^{-/-}$ mice (32). Another potential explanation is that $Pctp^{-/-}$ mice were more active than wild-type mice. However, physical activity when measured in individual cages at room temperature over a 24 h period was not statistically different and tended to be decreased for $Pctp^{-/-}$ mice (8). Because Pctp is also highly expressed in other oxidative tissues (10), non-Ucp1-dependent thermogenesis in tissues other than BAT could have contributed to the body temperatures observed for mice lacking Pctp. Finally, an important constraint of our study is that thermal challenges were limited to 24 h periods, which may not have been sufficient to achieve steady state in these mice.

Because of these potentially confounding influences, the in vivo findings were complemented by studies of brown adipocytes cultured from wild-type and $Pctp^{-/-}$ mice. Notwithstanding lower mRNA levels of Ucp1, as well as Pgc1a, Ppara, Tfam, and Nrf1 values of OCR were increased more robustly in response to norepinephrine stimulation in brown adipocytes cultured from $Pctp^{-/-}$ compared with wild-type mice. This did not appear to be a generalized effect because we did not observe a different response to insulin (33).

Taken together, our observations suggest that the absence of Pctp expression increases the intrinsic efficiency of thermogenesis in BAT and reduces the requirement for upregulation of thermogenic genes. Such an effect would be consistent with the hypothesis that Pctp limits the access of fatty acids to mitochondria by activating Them2 (8, 10), so that the absence of Pctp may have increased entry of fatty acids. Considering that they play a key role in activating Ucp1 (34), increased entry of fatty acids into mito-

chondria may have allowed not only increased oxidation but also increased specific activity of Ucp1.

The ultrastructural changes in brown fat of $Pctp^{-/-}$ mice appear to be in line with the proposed role for Pctp in limiting fatty acid oxidation, although our data do not exclude the possibility that the phosphatidylcholine transfer activity of Pctp (6) may have led to the observed changes, possibly by altering membrane composition. In the absence of Pctp expression, the increase in size of mitochondria in mature brown adipocytes is consistent with increased capacity for thermogenesis. However, increased β-oxidation of fatty acyl-CoA molecules can also be associated with physical damage to mitochondria by fatty acids or fatty acyl-CoA molecules (35) and by oxidative stress (36, 37). This could hasten cell death (36) and may have accounted for the degenerating mature brown adipocytes observed in $Pctp^{-/-}$ mice. The abundance of maturing and degenerating cells in brown fat from $Pctp^{-/-}$ mice could also explain why citrate synthase activity was not increased in proportion to mitochondrial size. This is because citrate synthase activity in a tissue homogenate reflects average total mass of mitochondria in all different cell types, not only the mature brown adipocytes that harbor enlarged mitochondria. It is also possible that the larger mitochondria were present in brown adipocytes of $Pctp^{-/-}$ mice at lower density, a parameter that was not captured by our analysis.

The capacity for BAT to sustain increases in thermogenesis despite ongoing mitochondrial damage and cell death appears to be explained by higher turnover of brown fat, as reflected by the abundant presence of developing brown adipocytes forms (i.e., protoadipocytes and preadipocytes). Although cultured brown adipocytes lacking Pctp appeared normal, gene expression during differentiation differed from wild-type cells. The relative changes in expression of Pparg, Pgc1a, and Ppara mRNA levels suggest that Pctp influenced the transcriptional control of differentiation. This notion is supported by the observation that reintroduction of Pctp early but not later during differentiation nearly restored the normal induction of these transcription factors.

When taken in context with prior observations in $Pctp^{-/-}$ mice, this study supports the assertion that Pctp limits brown fat-mediated thermogenesis by regulating energy substrate utilization. Evidence that phosphorylation by PKC promotes mitochondrial association of Pctp (9) suggests a potential mechanism. In addition to activating triglyceride hydrolysis, β_3-adrenergic stimulation of brown adipocytes leads to activation of PKC when PKA stimulates phosphatidylinositol 3-kinase (38). Under these conditions, activation of Them2 by translocation of Pctp to mitochondria would be expected to reduce fatty acid utilization. Considering that increased activity of brown fat appears to play an important role in reducing human body weight (14–16), inhibition of Pctp using small molecule inhibitors (39) could provide a route for the pharmacologic management of obesity.

REFERENCES

1. Ponting, C. P., and L. Aravind. 1999. START: a lipid-binding domain in StAR, HD-ZIP and signalling proteins. *Trends Biochem. Sci.* **24:** 130–132.

2. Roderick, S. L., W. W. Chan, D. S. Agate, L. R. Olsen, M. W. Vetting, K. R. Rajashankar, and D. E. Cohen. 2002. Structure of human phosphatidylcholine transfer protein in complex with its ligand. *Nat. Struct. Biol.* **9:** 507–511.

3. Alpy, F., and C. Tomasetto. 2005. Give lipids a START: the StAR-related lipid transfer (START) domain in mammals. *J. Cell Sci.* **118:** 2791–2801.

4. Soccio, R. E., and J. L. Breslow. 2003. StAR-related lipid transfer (START) proteins: mediators of intracellular lipid metabolism. *J. Biol. Chem.* **278:** 22183–22186.

5. Tsujishita, Y., and J. H. Hurley. 2000. Structure and lipid transport mechanism of a StAR-related domain. *Nat. Struct. Biol.* **7:** 408–414.

6. Wirtz, K. W. 1991. Phospholipid transfer proteins. *Annu. Rev. Biochem.* **60:** 73–99.

7. Kanno, K., M. K. Wu, E. F. Scapa, S. L. Roderick, and D. E. Cohen. 2007. Structure and function of phosphatidylcholine transfer protein (PC-TP)/StarD2. *Biochim. Biophys. Acta.* **1771:** 654–662.

8. Scapa, E. F., A. Pocai, M. K. Wu, R. Gutierrez-Juarez, L. Glenz, K. Kanno, H. Li, S. Biddinger, L. A. Jelicks, L. Rossetti, et al. 2008. Regulation of energy substrate utilization and hepatic insulin sensitivity by phosphatidylcholine transfer protein/StarD2. *FASEB J.* **22:** 2579–2590.

9. de Brouwer, A. P., J. Westerman, A. Kleinnijenhuis, L. E. Bevers, B. Roelofsen, and K. W. A. Wirtz. 2002. Clofibrate-induced relocation of phosphatidylcholine transfer protein to mitochondria in endothelial cells. *Exp. Cell Res.* **274:** 100–111.

10. Kanno, K., M. K. Wu, D. A. Agate, B. K. Fanelli, N. Wagle, E. F. Scapa, C. Ukomadu, and D. E. Cohen. 2007. Interacting proteins dictate function of the minimal START domain phosphatidylcholine transfer protein/StarD2. *J. Biol. Chem.* **282:** 30728–30736.

11. Mootha, V. K., J. Bunkenborg, J. V. Olsen, M. Hjerrild, J. R. Wisniewski, E. Stahl, M. S. Bolouri, H. N. Ray, S. Sihag, M. Kamal, et al. 2003. Integrated analysis of protein composition, tissue diversity, and gene regulation in mouse mitochondria. *Cell.* **115:** 629–640.

12. Wei, J., H. W. Kang, and D. E. Cohen. 2009. Thioesterase superfamily member 2 (Them2)/acyl-CoA thioesterase 13 (Acot13): a homotetrameric hotdog fold thioesterase with selectivity for long chain fatty acyl-CoAs. *Biochem. J.* **421:** 311–322.

13. Cannon, B., and J. Nedergaard. 2004. Brown adipose tissue: function and physiological significance. *Physiol. Rev.* **84:** 277–359.

14. Cypess, A. M., S. Lehman, G. Williams, I. Tal, D. Rodman, A. B. Goldfine, F. C. Kuo, E. L. Palmer, Y. H. Tseng, A. Doria, et al. 2009. Identification and importance of brown adipose tissue in adult humans. *N. Engl. J. Med.* **360:** 1509–1517.

15. van Marken Lichtenbelt, W. D., J. W. Vanhommerig, N. M. Smulders, J. M. Drossaerts, G. J. Kemerink, N. D. Bouvy, P. Schrauwen, and G. J. Teule. 2009. Cold-activated brown adipose tissue in healthy men. *N. Engl. J. Med.* **360:** 1500–1508.

16. Virtanen, K. A., M. E. Lidell, J. Orava, M. Heglind, R. Westergren, T. Niemi, M. Taittonen, J. Laine, N. J. Savisto, S. Enerback, et al. 2009. Functional brown adipose tissue in healthy adults. *N. Engl. J. Med.* **360:** 1518–1525.

17. Feldmann, H. M., V. Golozoubova, B. Cannon, and J. Nedergaard. 2009. UCP1 ablation induces obesity and abolishes diet-induced thermogenesis in mice exempt from thermal stress by living at thermoneutrality. *Cell Metab.* **9:** 203–209.

18. de Jesus, L. A., S. D. Carvalho, M. O. Ribeiro, M. Schneider, S. W. Kim, J. W. Harney, P. R. Larsen, and A. C. Bianco. 2001. The type 2 iodothyronine deiodinase is essential for adaptive thermogenesis in brown adipose tissue. *J. Clin. Invest.* **108:** 1379–1385.

19. Uldry, M., W. Yang, J. St-Pierre, J. Lin, P. Seale, and B. M. Spiegelman. 2006. Complementary action of the PGC-1 coactivators in mitochondrial biogenesis and brown fat differentiation. *Cell Metab.* **3:** 333–341.

20. Geloen, A., A. J. Collet, G. Guay, and L. J. Bukowiecki. 1990. In vivo differentiation of brown adipocytes in adult mice: an electron microscopic study. *Am. J. Anat.* **188:** 366–372.

21. He, D., S. J. Hagen, C. Pothoulakis, M. Chen, N. D. Medina, M. Warny, and J. T. LaMont. 2000. Clostridium difficile toxin A causes early damage to mitochondria in cultured cells. *Gastroenterology.* **119:** 139–150.

22. Rockl, K. S., M. F. Hirshman, J. Brandauer, N. Fujii, L. A. Witters, and L. J. Goodyear. 2007. Skeletal muscle adaptation to exercise training: AMP-activated protein kinase mediates muscle fiber type shift. *Diabetes.* **56:** 2062–2069.

23. Elchalal, U., W. T. Schaiff, S. D. Smith, E. Rimon, I. Bildirici, D. M. Nelson, and Y. Sadovsky. 2005. Insulin and fatty acids regulate the expression of the fat droplet-associated protein adipophilin in primary human trophoblasts. *Am. J. Obstet. Gynecol.* **193:** 1716–1723.

24. da-Silva, W. S., J. W. Harney, B. W. Kim, J. Li, S. D. Bianco, A. Crescenzi, M. A. Christoffolete, S. A. Huang, and A. C. Bianco. 2007. The small polyphenolic molecule kaempferol increases cellular energy expenditure and thyroid hormone activation. *Diabetes.* **56:** 767–776.

25. Scarpulla, R. C. 2008. Transcriptional paradigms in mammalian mitochondrial biogenesis and function. *Physiol. Rev.* **88:** 611–638.

26. van Helvoort, A., A. de Brouwer, R. Ottenhoff, J. F. Brouwers, J. Wijnholds, J. H. Beijnen, A. Rijneveld, T. van der Poll, M. A. van der Valk, D. Majoor, et al. 1999. Mice without phosphatidylcholine transfer protein have no defects in the secretion of phosphatidylcholine into bile or into lung airspaces. *Proc. Natl. Acad. Sci. USA.* **96:** 11501–11506.

27. Nagy, T. R., D. Krzywanski, J. Li, S. Meleth, and R. Desmond. 2002. Effect of group vs. single housing on phenotypic variance in C57BL/6J mice. *Obes. Res.* **10:** 412–415.

28. Himms-Hagen, J., and C. Villemure. 1992. Number of mice per cage influences uncoupling protein content of brown adipose tissue. *Proc. Soc. Exp. Biol. Med.* **200:** 502–506.

29. Riachi, M., J. Himms-Hagen, and M. E. Harper. 2004. Percent relative cumulative frequency analysis in indirect calorimetry: application to studies of transgenic mice. *Can. J. Physiol. Pharmacol.* **82:** 1075–1083.

30. Puigserver, P., and B. M. Spiegelman. 2003. Peroxisome proliferator-activated receptor-gamma coactivator 1 alpha (PGC-1 alpha): transcriptional coactivator and metabolic regulator. *Endocr. Rev.* **24:** 78–90.

31. Evans, R. M., G. D. Barish, and Y. X. Wang. 2004. PPARs and the complex journey to obesity. *Nat. Med.* **10:** 355–361.

32. Seale, P., B. Bjork, W. Yang, S. Kajimura, S. Chin, S. Kuang, A. Scime, S. Devarakonda, H. M. Conroe, H. Erdjument-Bromage, et al. 2008. PRDM16 controls a brown fat/skeletal muscle switch. *Nature.* **454:** 961–967.

33. Omatsu-Kanbe, M., M. J. Zarnowski, and S. W. Cushman. 1996. Hormonal regulation of glucose transport in a brown adipose cell preparation isolated from rats that shows a large response to insulin. *Biochem. J.* **315:** 25–31.

34. Rial, E., and M. M. Gonzalez-Barroso. 2001. Physiological regulation of the transport activity in the uncoupling proteins UCP1 and UCP2. *Biochim. Biophys. Acta.* **1504:** 70–81.

35. Singh, A. K., Y. Yoshida, A. J. Garvin, and I. Singh. 1989. Effect of fatty acids and their derivatives on mitochondrial structures. *J. Exp. Pathol.* **4:** 9–15.

36. Orrenius, S., V. Gogvadze, and B. Zhivotovsky. 2007. Mitochondrial oxidative stress: implications for cell death. *Annu. Rev. Pharmacol. Toxicol.* **47:** 143–183.

37. Savitha, S., and C. Panneerselvam. 2006. Mitochondrial membrane damage during aging process in rat heart: potential efficacy of L-carnitine and DL alpha lipoic acid. *Mech. Ageing Dev.* **127:** 349–355.

38. Chernogubova, E., B. Cannon, and T. Bengtsson. 2004. Norepinephrine increases glucose transport in brown adipocytes via beta3-adrenoceptors through a cAMP, PKA, and PI3-kinase-dependent pathway stimulating conventional and novel PKCs. *Endocrinology.* **145:** 269–280.

39. Wagle, N., J. Xian, E. Y. Shishova, J. Wei, M. A. Glicksman, G. D. Cuny, R. L. Stein, and D. E. Cohen. 2008. Small-molecule inhibitors of phosphatidylcholine transfer protein/StarD2 identified by high-throughput screening. *Anal. Biochem.* **383:** 85–92.